

Comprehensive Analytical and Experimental Analysis of a Self Excited Induction Generator for Renewable Energy Application

M. Faisal Khan^{*‡}, M. Rizwan Khan^{**}

* Electrical Engineering Section, University Polytechnic Faculty of Engineering. & Technology, Aligarh Muslim University, Aligarh - 202002, UP, India

**Electrical Engineering Department, Zakir Husain College of Engineering & Technology, Aligarh Muslim University, Aligarh - 202002, UP, India

(mfaisal_khan@yahoo.com, rizwan.eed@gmail.com)

‡Corresponding Author; M. Faisal Khan, Tel: +91 9897439890, mfaisal_khan@yahoo.com

Received: 11.04.2015 Accepted:24.05.2015

Abstract-Self excited induction generators have attracted a lot of interest from the researchers in recent past. The main focus in this regard has been on modeling techniques and their verification. Such analyses are invariably restricted exclusively either to dynamic or steady state characteristic evaluation. The objective of this paper is to highlight the operational features of self excited induction generators through detailed experimental results. For analytical verification steady state and dynamic models are implemented through symbolic programming and Simulink modeling approaches respectively. Diverse set of static loads of different power factors as well as dynamic loading is employed to carry out power quality analysis of SEIG on a Fluke 435 II power quality and energy analyzer to conclude the paper. The tests are carried out on an open stator winding, squirrel caged induction motor operated as SEIG.

Keywords Self excited induction generator, Steady state, Dynamic, Variable power factor, Dynamic load.

Nomenclature

Symbol	Description	Symbol	Description
R_s, R_r, R_L	stator, rotor and load resistances (ohms)	P_o	active power generated (watts)
L_{sl}, L_{rl}	stator & rotor leakage inductances (henry)	Q_c	reactive power (var)
Ψ_{sd}, Ψ_{sq}	d and q axes stator flux(wb)	C_{ex}	shunt or excitation capacitance(μ F)
Ψ_{rd}, Ψ_{rq}	d and q axes rotor flux(wb)	C_{se}	series or compensation capacitance(μ F)
Ψ_{rd0}, Ψ_{rq0}	d and q axes initial rotor flux(wb)	Ψ_m	magnetizing flux (wb)
V_{dcap}, V_{qcap}	d and q axes instantaneous voltages across excitation capacitance (volts).	V_{rd0}, V_{rq0}	d and q axes rotor induced voltages due to remnant flux(volts)
V_{dcse}, V_{qcse}	d and q axes instantaneous voltages across series capacitance (volts).	X_{ex}	reactance of capacitance reactance(ohms)
V_{dcap0}, V_{qcap0}	d and q axes voltages due to initial charge on excitation capacitance(volts).	X_{se}	reactance of series capacitance(ohms)
V_T	terminal voltage(volts)	X_m	magnetizing reactance(ohms)
V_L	load voltage (volts)	X_L	load reactance(ohms)
ω_r	rotor electrical speed(rads/sec)	Z_L	load impedance(ohms)
L_m	magnetizing inductance (henry)	f_{pu}	per unit generation frequency(Hz)
L_L	load inductance (henry)	T_e	Electromagnetic Torque (Nm)
I_L	load Current(amps)	i_{dcap}, i_{qcap}	d and q axes capacitor currents(amps)
I_s	stator current(amps)	i_{sd}, i_{sq}	d and q axes stator currents(amps)
I_m	magnetizing current(amps)	i_{rd}, i_{rq}	d and q axes rotor currents(amps)
I_c	excitation capacitor current(amps)	i_{Ld}, i_{Lq}	d and q axes load currents(amps)

1. Introduction

The global energy scenario has experienced thrust over last two decades towards new and renewable energy generation [1,2]. Based on different modeling approaches a number of steady state analyses are reported on SEIGs [3]-[7]. All these approaches are implemented to yield two non-linear equations which are then solved for two unknowns which are invariably in terms of generation frequency (f_{pu}) and magnetizing reactance (X_m).

Steady state models presented in [4] and [5] are deduced by non-linear equations through loop impedance based equivalent circuits. Chan in [4] proposed two iterative technique based methods; first is realized by numerical solution of a 7th order non-linear equation and the second is implemented through symbolic programming. Haque in [5] has developed a switched capacitor scheme for constant terminal voltage and stator current operation through an optimization tool based technique that completely avoids iterative approach.

Branch admittance based approach [6,7] is another widely used modeling methodology for SEIGs. Chan in [6] has developed steady state model of SEIG in terms of admittances connected across its magnetizing circuit by iterative technique based solution. In [7] a composite model of SEIG including the saturation of transformer supplying the load circuit through branch admittance approach is developed.

Dynamic modeling of induction machines in d-q axes in different frames of reference is well documented [8]. The same is employed for generation mode with necessary modifications [9]-[11]. In [9] Grantham has developed a transient model of SEIG in stationary frame of reference to analyze self excitation process. Seyoum in [10] developed a d-q model in stationary reference frame to study the effects of magnetizing inductance on the dynamic performance of SEIG driven by a wind turbine. Bulk power augmentation is necessary for any generation regime and is invariably achieved through parallel operation of generators. The parallel operation of two SEIGs is presented in [11] through the dynamic model of the system.

A known operational drawback of SEIGs is an inherently poor voltage regulation [12]. This obviously renders them extremely restrictive in-terms of practical applications. Many remedies are proposed to deal with this issue. Of these some deploy power electronic devices such as SVC [13], STATCOM [14], DSTATCOM [15] etc., for constant voltage and frequency operation. While others [16] suggest switched capacitor schemes where in the optimum capacitance is switched in the SEIG circuit. However, the switching devices entrusted to implement the requisite control schemes induce transients giving rise to PQ issues and adversely affect the ruggedness of the system on the whole.

In spite of a number of good quality studies available on SEIGs in the literature as discussed above, majority of them are specific in nature *vis-à-vis* either steady state or

transient analyses. Those incorporating both models [9] are very specific in their scope.

This paper addresses the aforementioned issues by carrying out a comprehensive study on an open stator winding SEIG. Unlike usual approach of theoretical analysis verified by experimental tests, the present work encompasses an exhaustive set of experimental results representing both steady state and dynamic responses of SEIG. The analytical models are developed through symbolic programming approach and Simulink modeling both implemented through MATLAB [17].

In the present study more robust, simple but effective technique of series compensation through static capacitor [18,19] connected in short shunt configuration is adopted. The performance of SEIG is tested on static loads of variable power factor as well as dynamic load in the form of a three phase induction motor. The self compensated SEIG model is able to carry all types of loading without any major issues.

2. Self Excited Induction Generators for Renewable Energy Application

Self excited induction generators are identified as fixed speed or type 1 wind turbine generators [2]. They are squirrel caged induction machines operated in generation mode and can supply power as an isolated as well as grid connected unit. The biggest attributes of SEIGs are that they are extremely rugged, maintenance free, economical and possess an inherent ability of self protection against short circuits and over loads as the excitation breaks down immediately under such transient conditions [3]. These are the main reasons of their large scale deployment in wind energy conversion systems as such installations are invariably located in hostile environment in the peripheral or far off places.

Their main disadvantage is that they do not generate reactive power rather consume it and hence have an inherently poor voltage regulation. Thus, reactive power requirements of SEIGs to supply excitation as well as the loads they feed have to be met through some external means. When operating in standalone mode which is the focus of this paper their reactive power requirement is fulfilled by terminal capacitors. A general purpose induction motor of required variant (1 phase, 3 phase) and rating can be easily customized to act as a SEIG generator.

3. SEIG Modeling and Description

A basic SEIG system implemented through a three phase induction motor is illustrated in Fig. 1. In order to realize SEIG performance two models in-terms of dynamic d-q in stationary reference frame and per phase steady state are developed to carry out detailed analytical study.

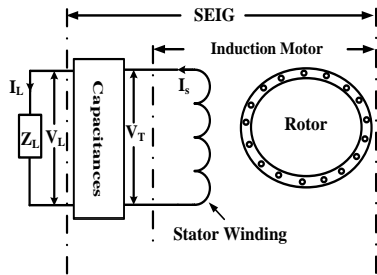


Fig. 1. Basic Implementation of SEIG system.

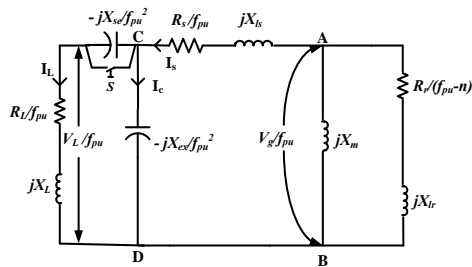


Fig. 2. Per phase steady state equivalent circuit of SEIG.

3.1. Steady State Modeling and Performance Analysis of SEIG

The steady state analysis of SEIG in the context of this paper is referred to the study of its output characteristics subsequent to rated voltage build-up. The steady state analysis yields variation of different SEIG parameters over the entire output power range. The per phase equivalent circuit of a SEIG in self compensated short shunt connection is depicted in Fig. 2. The KVL equation incorporating various impedances of the circuit may be written as:

$$I_s (Z_{CA} + Z_{CD} + Z_{AB}) = 0. \tag{1}$$

Where,

$$Z_{CA} = R_s / f_{pu} + jX_s$$

$$Z_{CD} = (-jX_{ex} / f_{pu}^2) \parallel (R_L / f_{pu} + j(X_L - X_{se}))$$

$$Z_{AB} = (jX_m) \parallel (R_r / (f_{pu} - n) + jX_r)$$

For the successful voltage buildup of SEIG the stator current, I_s must not be equal to zero. Therefore, from Eq. (1) the following expression is obtained.

$$(Z_{CA} + Z_{CD} + Z_{AB}) = 0 \tag{2}$$

If the real and imaginary parts of Eq. (2) are separately equated to zero, two equations in-terms of per unit frequency, f_{pu} and the magnetizing reactance X_m , are obtained as follows [4,20]:

$$\alpha_7 f_{pu}^7 + \alpha_6 f_{pu}^6 + \alpha_5 f_{pu}^5 + \alpha_4 f_{pu}^4 + \alpha_3 f_{pu}^3 + \alpha_2 f_{pu}^2 + \alpha_1 f_{pu} + \alpha_0 = 0 \tag{3}$$

Modified constants α_0 - α_7 for short shunt mode of operation are given in [19].

$$X_m = \left\{ \frac{(X_{ls} - Z_{CDi})^2 + ((Z_{CDr} + (R_s / f_{pu}))^2)}{(X_{lr}^2 + (R_r / (f_{pu} - n))^2)} \right\} / \left\{ \frac{(Z_{CDi} - X_{ls})(X_{lr}^2 + (R_r / (f_{pu} - n))^2) - X_{lr}((X_{ls} - Z_{CDi})^2 + ((Z_{CDr} + (R_s / f_{pu}))^2))}{(X_{ls} - Z_{CDi})^2 + ((Z_{CDr} + (R_s / f_{pu}))^2)} \right\} \tag{4}$$

Where,

$$Z_{CDr} = \text{Re}\{Z_{CD}\}$$

$$Z_{CDi} = \text{Im}\{Z_{CD}\}$$

Under operating conditions the difference between per unit frequency, f_{pu} and the per unit speed, n of a SEIG is

negligible [21,22]. Considering, this practical aspect a parameter ζ may be defined as:

$$f_{pu} = \zeta + n \tag{5}$$

Where, ζ is a very small value, thus from above the per unit frequency, f_{pu} may be replaced in Eq. (3) by the following new expression.

$$f_{pu} = \zeta + n \tag{6}$$

Further considering the fact that values of ζ^x for all $x > 2$ shall be negligibly small; all such values can be neglected. Thus by putting f_{pu} from Eq. (6) in Eq. (3) following quadratic in terms of ζ [20] is obtained:

$$B_2 \zeta^2 + B_1 \zeta + B_0 = 0 \tag{7}$$

From (7), the parameter ζ may be calculated as follows:

$$\zeta = - \frac{(B_1 - \sqrt{B_1^2 - 4B_2B_0})}{2B_2} \tag{8}$$

Constants B_0 - B_2 for short shunt SEIG are defined in [19].

Knowing the value of ζ , the task of calculating f_{pu} becomes straightforward from Eq. (6) for a given per unit speed, n .

Putting the calculated f_{pu} in Eq. (4), X_m can be found for the given loading condition.

The performance equations are given as;

$$I_s = \frac{V_g}{f_{pu} (Z_{CA} + Z_{CD})} \tag{9}$$

$$I_L = \frac{-j \frac{X_{ex}}{f_{pu}^2}}{\frac{R_L}{f_{pu}} + j \left(X_L - \frac{X_{ex}}{f_{pu}^2} \right)} I_s \tag{10}$$

$$V_t = f_{pu} I_L Z_L \tag{11}$$

$$P_{out} = 3 I_L^2 R_L \tag{12}$$

The performance Eqns. (9) to (12) can only be solved if the air gap voltage V_g is known. For this analysis the V_g / f_{pu} i.e. air gap voltage normalized to base frequency for different ranges of magnetizing reactance (X_m) is evaluated through synchronous speed test of the motor [23]. The relationship is formulated in terms of magnetizing characteristic given in Appendix-I

$$\tag{3}$$

3.2. Selection of Optimum Capacitances

An optimum excitation capacitance facilitates generation of rated no-load voltage across SEIG terminals when it is driven at rated speed. For investigated machine variation of no-load generated voltage with respect to different excitation capacitances is plotted in Fig. 3. For simulation Z_L i.e. load impedance is kept constant at very high value and excitation capacitance is varied keeping all other parameters constant as well. The characteristic clearly suggests that an excitation capacitance of 12.5 μF gives

optimum SEIG no-load voltage of 240 V. The external characteristics of SEIG without and with different series capacitances and optimum excitation capacitance are shown in Fig 4. When no series compensation is facilitated the SEIG output voltage profile is expectedly poor. The gross output power generated by SEIG under this mode of operation is 590 W that is about 26 % of the machine rating at a full load voltage regulation of 20 %.

For self compensated mode of operation SEIG performance is assessed with different set of series capacitances of 30 μ F, 40 μ F, 70 μ F. It is evident from Fig. 4 that 40 μ F capacitance in each of the three phases of load windings enables the SEIG to maintain most optimum performance. This series capacitance is able to maintain load voltage within ± 6.9 % of the no-load voltage over the entire output power range which is acceptable. Whereas, the corresponding range for 70 μ F series capacitances is 16 %. It is also observed that 30 μ F series capacitance is unable to meet rated power demand. From this analysis it is found that a capacitance of 40 μ F in series with each phase yields best load voltage profile. Thus, for further analysis 12.5 μ F and 40 μ F are selected as optimum excitation and series capacitance combination.

Details and an illustration of three phase SEIG test rig is given in Appendix-II

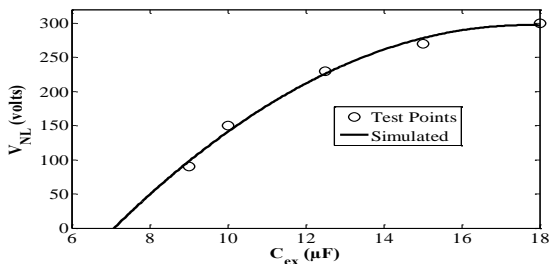


Fig. 3. Measured and simulated variation of no-load voltage with excitation capacitance.

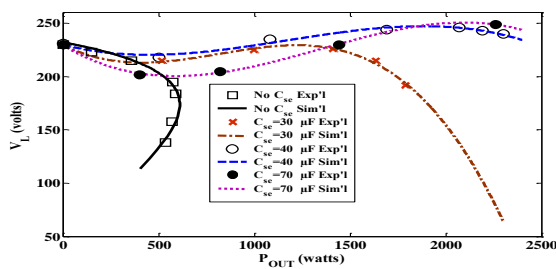


Fig. 4. External characteristics of SEIG without and with different series.

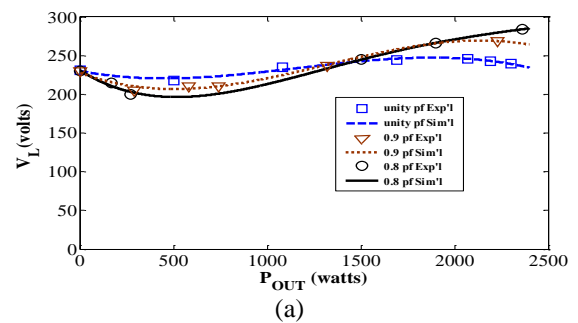
3.3. Steady State Load Performance of SEIG

Subsequent to selection of optimum series capacitance the SEIG is subjected to loads of different power factors. Fig. 5(a) shows the load voltage profile for each of the three power factors considered. The result for unity pf need no further elaboration as it has already been discussed in the last section. For both lagging power factors of 0.9 and 0.8 the terminal load voltage profiles are sagging in nature. Also, for

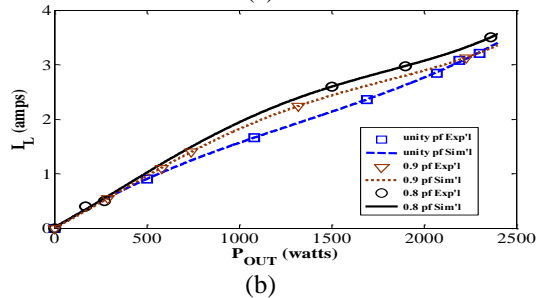
lagging loads the terminal load voltage corresponding to full load is increasing with decreasing power factor. This is a consequence of series resonance of the SEIG's load winding equipped with R_L - L_L - C_{se} parameters. The load voltage across lagging pf loads under goes three transitional states corresponding to pre-resonance, during resonance and post-resonance conditions. In the first region voltage keeps decreasing with load as $X_L > X_{se}$ and attains a minima corresponding to resonating condition where $X_L = X_{se}$. Afterwards, as the load impedance and hence X_L and R_L both are decreased to increase loading the X_L becomes less than X_{se} which indicates over compensation and hence the load voltage increases. Load currents plotted in Fig. 5(b) further confirm this proposition as the 'bow' shaped profiles for lagging pf loads exhibit increase in current corresponding to resonating region and gradual decrease in post-resonance or overcompensation region.

The SEIG terminal voltages and stator currents for different power factors are plotted in Fig. 6(a) and Fig. 6(b) respectively. It is important to keep the stator current within 5.5 A i.e. the current rating of present motor, which is easily maintained for all three power factors in the present case. An increase in stator current beyond motor rating will cause overheating and eventual damage to the motor employed as SEIG.

The SEIGs besides an inherently poor voltage regulation also carry drooping frequency characteristic [24]. It is evident from the Fig. 7 where in for each power factor the frequency is gradually dropping with load power. It is unacceptable for grid integration unless suitable controllers are employed to pull back the frequency to the rated value of 50 Hz. However, in standalone/isolated mode of operation the SEIGs feed mostly lighting and heating loads which are frequency insensitive. Therefore, in present analysis no attempt is made to regulate the frequency.



(a)



(b)

Fig. 5. Generated voltages corresponding to load power at different power factors of SEIG (a) terminal load voltage (b) load current.

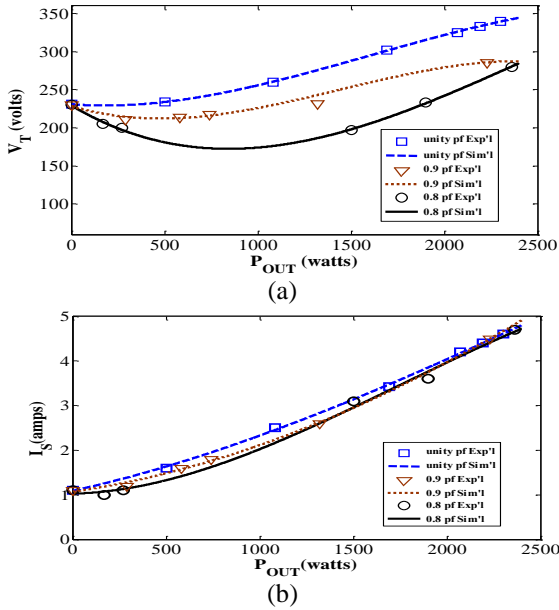


Fig. 6. Variation of generated currents with output power at different power factor loads (a) terminal voltage (b) stator currents.

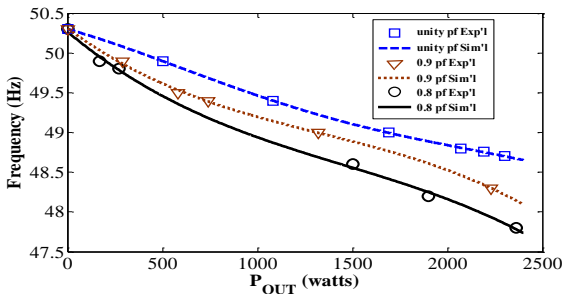


Fig. 7. Variation of frequency with output power

4. Dynamic Modeling and Performance Analysis

The d-q model of a short shunt SEIG in stationary reference frame incorporating various flux linkages is depicted in Fig. 8.

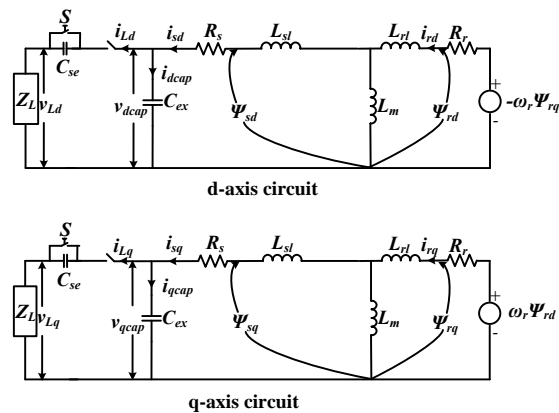


Fig. 8. d-q model of a three phase SEIG in stationary reference frame.

The model is essentially based on non-compensated model of SEIG presented by Seyoum in [10]. However, for

the present study necessary modifications are incorporated to include the affect of series capacitance and R-L load models. The entire model can be formulated in a single state space equation of the form given by Eq. (13) as follows.

$$[K][i]^T + [L]p[i]^T + [v]^T = 0 \tag{13}$$

where,

$$p = d/dt; [v] = [v_{qcap} \quad v_{dcap} \quad v_{rq0} \quad v_{rd0}]^T;$$

$$[i] = [i_{sq} \quad i_{sd} \quad i_{rq} \quad i_{rd}]^T; [L] = \begin{bmatrix} L_s & 0 & L_m & 0 \\ 0 & L_s & 0 & L_m \\ L_m & 0 & L_r & 0 \\ 0 & L_m & 0 & L_r \end{bmatrix}$$

$$[K] = \begin{bmatrix} R_s & 0 & 0 & 0 \\ 0 & R_s & 0 & 0 \\ 0 & -\omega_r L_m & R_r & -\omega_r L_r \\ \omega_r L_m & 0 & \omega_r L_r & R_r \end{bmatrix};$$

$$L_s = L_{sl} + L_m; L_r = L_{rl} + L_m; v_{rq0} = -\omega_r \Psi_{rq0}; v_{rd0} = \omega_r \Psi_{rd0}$$

$$p[i]^T = -[L]^{-1}[K][i]^T - [L]^{-1}[v]^T \tag{14}$$

The modelling of different SEIG parameters is given as:

Modeling of Excitation Capacitance:

$$v_{(qd)cap} = \frac{1}{C_{ex}} \int i_{(qd)cap} dt + v_{(qd)cap0} \tag{15}$$

above equation is expanded as:

$$v_{qcap} = \frac{1}{C_{ex}} \int i_{qcap} dt + v_{qcap0}$$

$$v_{dcap} = \frac{1}{C_{ex}} \int i_{dcap} dt + v_{dcap0}$$

the remaining equations are written in the similar manner.

Here, $i_{(qd)cap} = i_{s(qd)}$.

Modeling of Load:

Now, $i_{(qd)cap} = i_{s(qd)} - i_{L(qd)}$

$$v_{(qd)cap} = \frac{1}{C_{ex}} \int (i_{s(qd)} - i_{L(qd)}) dt + v_{(qd)cap0} \tag{16}$$

$$p i_{L(qd)} = \left(\frac{v_{(qd)cap}}{L_L} \right) - \left(\frac{R_L}{L_L} \right) i_{L(qd)} - \frac{1}{L_L C_{se}} \int (i_{L(qd)}) dt \tag{17}$$

$$v_{(qd)cse} = \frac{1}{C_{se}} \int i_{L(qd)} dt$$

$$v_{L(qd)} = v_{(qd)cap} - v_{(qd)cse}$$

$$T_e = 0.75 P_N L_m (i_{sd} i_{rq} - i_{sq} i_{rd}) \tag{18}$$

where, P_N : no. of poles.

4.1. Self Excitation and No-Load Voltage Buildup

Self excitation is a transient phenomenon which requires onset of transient excitation current increasing with time and facilitated by an initial charge either on the excitation capacitors or in the core.

The simulated and experimental voltage build-ups shown in Fig. 9 and Fig. 10 illustrate the dynamics of SEIG no-load voltage when the initial charge is derived from excitation capacitance and core respectively. For build-up initiated from excitation capacitance the charged capacitors are kept isolated from the SEIG terminals as it is brought up-to rated speed by prime mover. As soon as the SEIG gains rated speed of 1500 rpm the switch connecting the capacitors to SEIG terminals is closed to initiate self excitation. The instant of capacitor ‘switch on’ can be observed by a transient increase in generated voltage at the beginning of

measured result of Fig. 9. The terminal voltage increases rapidly eventually achieving steady state in the saturation region.

To analyze self excitation and voltage build-up initiated from remnant charge in machine rotor. The machine is first operated in motoring mode to set up remnant flux. The capacitances are discharged and kept isolated from SEIG terminals as its speed is brought up-to a 1500 rpm. Once running at rated speed the capacitances are switched on at the same instant as was done in the earlier case. Due to capacitors being discharged there is no initial impulse as there is no-crossover of charges from capacitances towards the machine. Rather the capacitances initially get charged from weak magnetizing current coming from the remnant flux of rotor. Afterwards, the voltage builds up smoothly as shown in Fig. 10 .

A comparison of both results suggests that voltage build-up and its stabilization takes place earlier when the self excitation is initiated from the excitation capacitances. As can be seen the generated voltage attains steady state in 1.1s for capacitance initiated build-up. While for rotor initiated build-up the voltage stabilizes in about 1.4s. Thus, it can be seen that voltage build-up initiated from remnant charge on excitation capacitance achieves steady state quicker as compared to when initiated from rotor side.

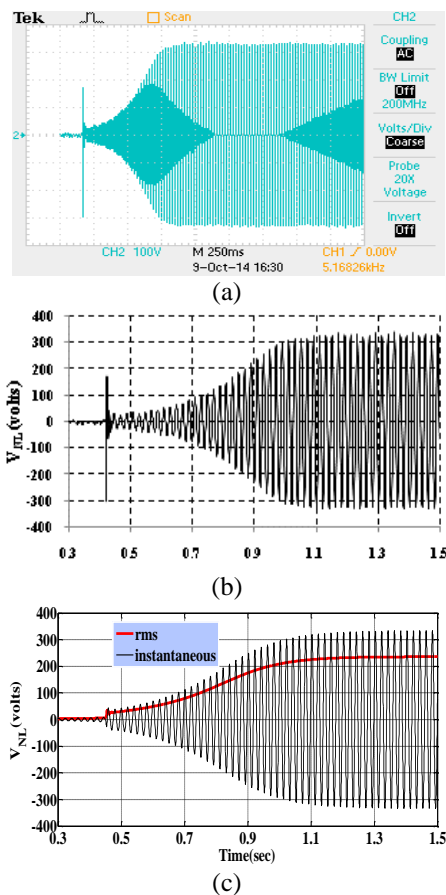


Fig. 9. Voltage build-up initiated by residual voltage from excitation capacitance(a) measured (b)plot from data file of measured result. (c) simulated.

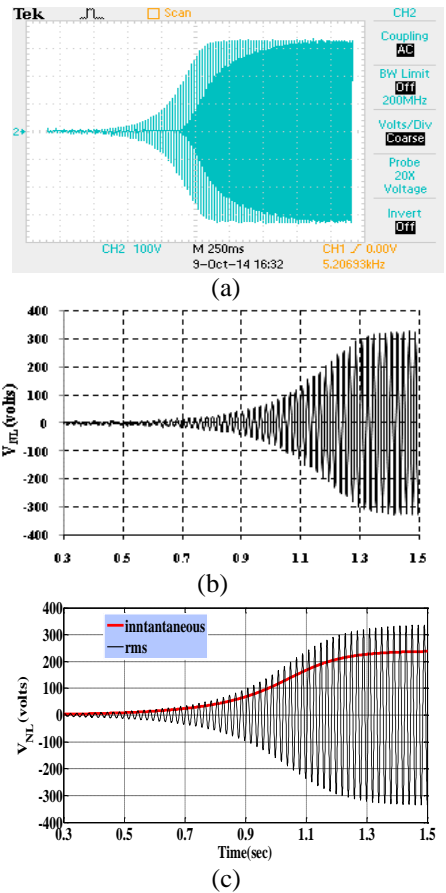


Fig. 10. Voltage build-up initiated by residual voltage from rotor (a) measured (b) plot from data file of measured result (c) simulated.

4.2. Load Analysis

The simulated and experimental loading transients of phase A of short shunt SEIG subjected to step loads of different power factors are illustrated in Fig. 11, Fig. 12 and Fig. 13. The response of SEIG for unity pf loading is shown in Fig. 11. It can be seen that series capacitance is able to maintain almost constant voltage post loading. The rising load voltages for 0.9 and 0.8 lagging power factors are depicted in Fig. 12 and Fig. 13 respectively.

The increasing load voltages for lagging power factors can be brought within permissible limit if series capacitance is switched in single stage. For present case the verification of such a strategy is done. It is found that if the series capacitance is switched from 40 μF to 25 μF the load voltages for both lagging power factors could be brought down. For 0.9 lagging power factor the switching causes load voltage to reduce to 220 V. The same results in full load voltage at 0.8 lagging power factor reducing to 235 V.

Thus, with single stage switching the full load voltage regulation of SEIG can be maintained within $\pm 5\%$ for all three power factors considered. A summary of simulated and measured SEIG parameters is given in Table 1.

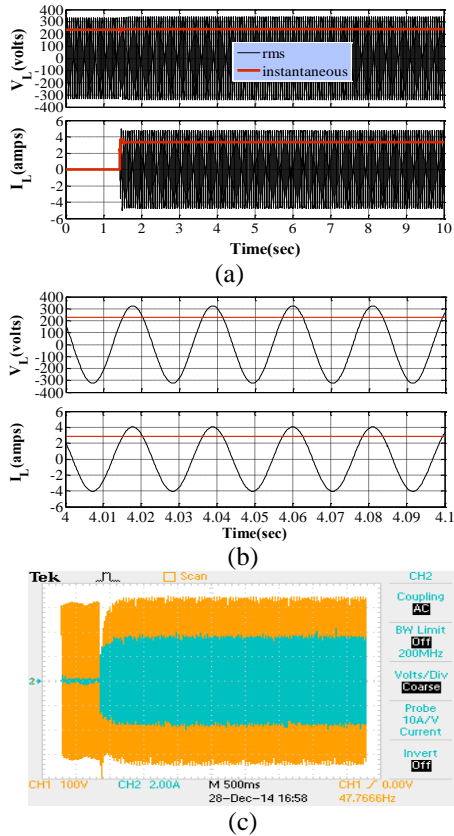


Fig. 11. Loading transients corresponding to unity power factor. (a) Simulated. (b) Zoomed load voltage and current. (c) Measured voltage (saffron) and current (sky blue).

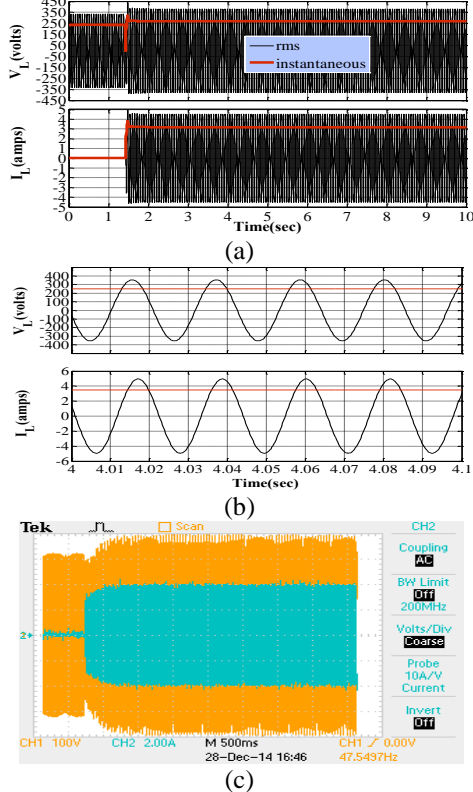


Fig. 12. Loading transients corresponding to 0.9 lagging power factor. (a) Simulated. (b) Zoomed load voltage and current. (c) Measured voltage (saffron) and current (sky blue).

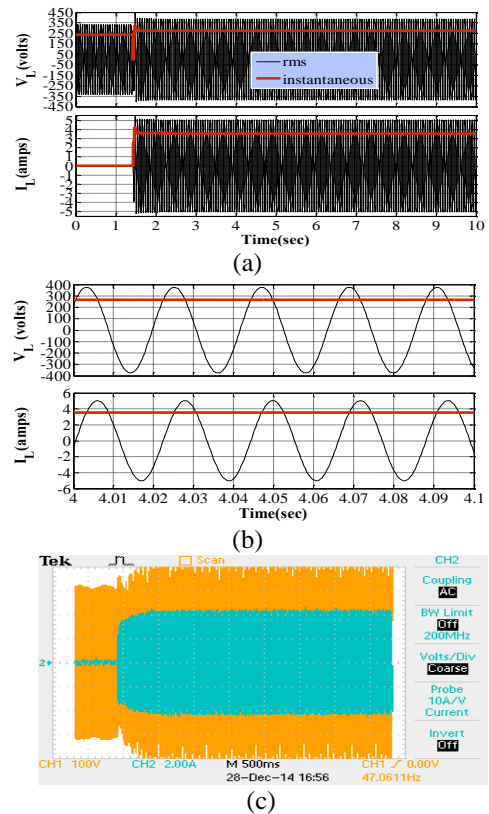


Fig. 13. Loading transients corresponding to 0.8 lagging power factor. (a) Simulated. (b) Zoomed load voltage and current. (c) Measured voltage (saffron) and current (sky blue).

Table 1. Experimental and Simulated parameters of SEIG

Type of Load	V_L (V)		I_L (A)	
	Sim'l	Exp'l	Sim'l	Exp'l
Unity PF	235	241	3.3	3.1
0.9 pf lagging	260	270	3.6	3.2
0.8 lagging	270	285	3.6	3.5

5. Power Quality (PQ) Analysis

Detailed study on the quality of generated parameters of SEIG is carried on a Fluke 435 II power quality and energy analyzer to experimentally monitor SEIG's response to different pf loadings. Results are depicted in Fig. 14, Fig. 15 and Fig. 16. Apart from the given static loads, the SEIG performance is also tested for dynamic load. Dynamic loads are highly non-linear in nature and operate at poor lagging power factors. In the present scenario a 3 phase, 1 hp induction motor is operated from the output of implemented SEIG. For the dynamic loading the series capacitance is changed to 15 μ F. This is needed because when operated with the erstwhile optimum series capacitance of 40 μ F the load voltage rises to very high value on switching the motor load. It so happens as the motor power factor is close to 0.4(lagging) as is evident from Fig. 17 and as observed with decreasing pfs the load voltage keeps increasing. Also, the motor could not be loaded till 1 hp due to this reason.

The imbalance in the three phase voltages as well as currents can be seen and is attributed to slight inaccuracies in the three phase R as well as L loads. The phasors of three phase voltages and currents show an almost perfect 120° angular displacements between respective voltages and respective currents for all conditions. Various measured output parameters of SEIG are given in Table 2.

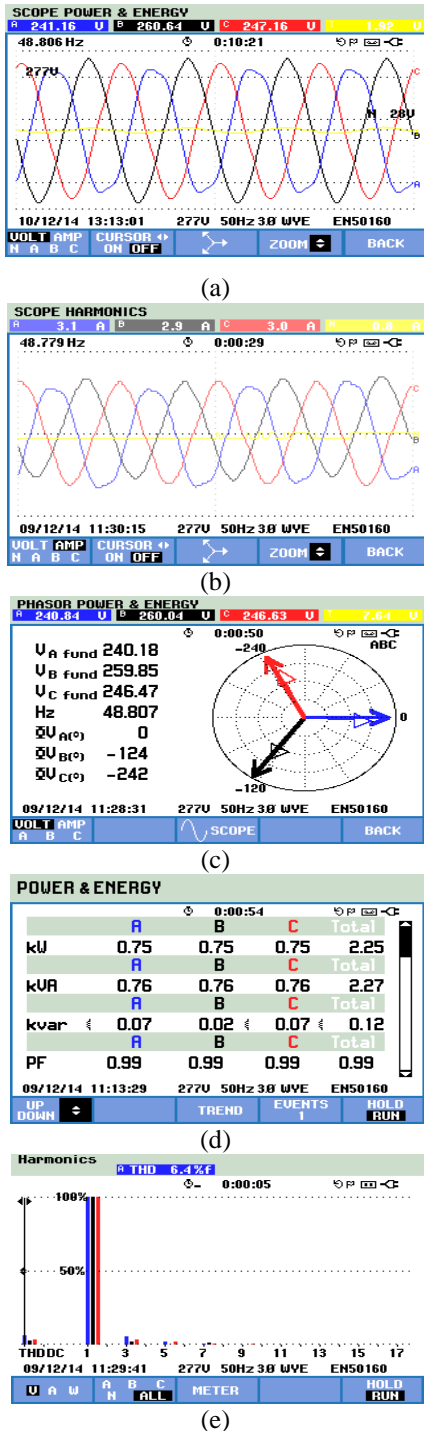


Fig. 14. Measured output parameters of SEIG supplying rated unity power factor load (a) three phase load voltages (b) three phase load currents (c) phasors of load voltage and currents (d) generated active, reactive and apparent powers and operational power factor (e) load voltage harmonics.

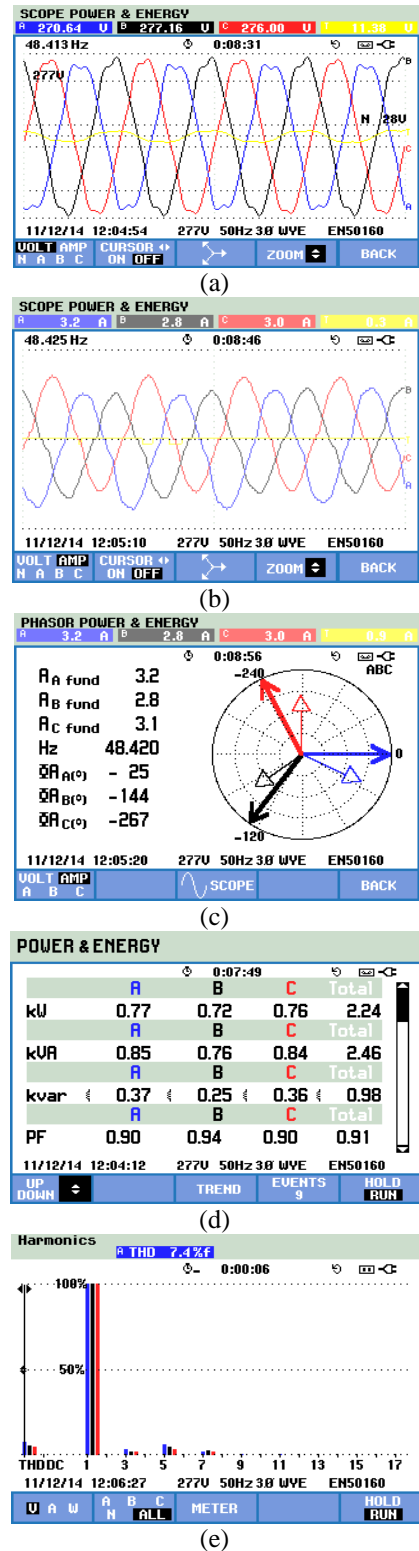
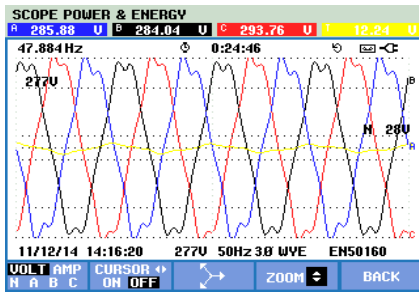
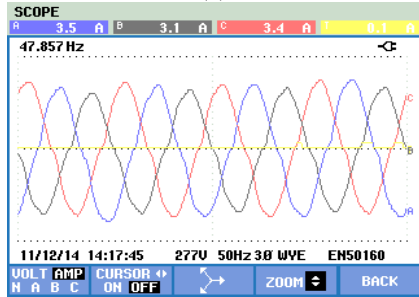


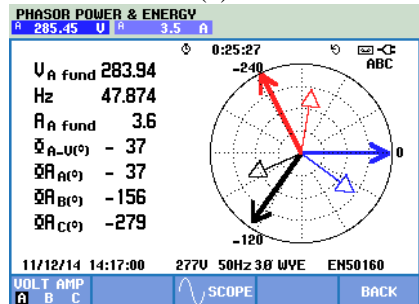
Fig. 15. Measured output parameters of SEIG at rated load of 0.9 lagging power factor (a) three phase terminal load voltages (b) three phase load currents (c) phasors of load voltage and currents (d) active, reactive and apparent powers and operational power factor (e) load voltage harmonics.



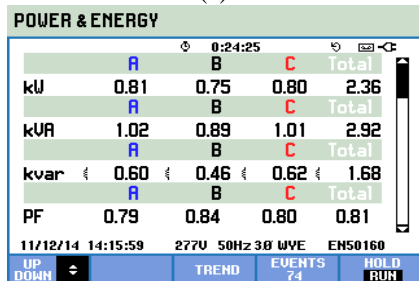
(a)



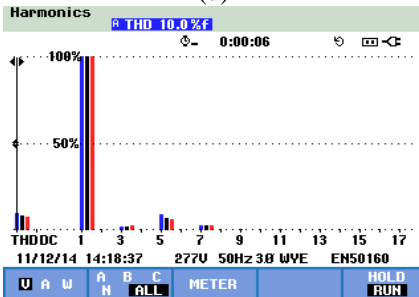
(b)



(c)

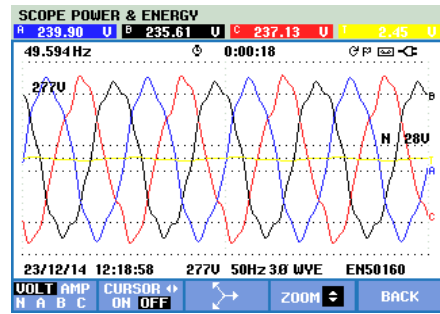


(d)

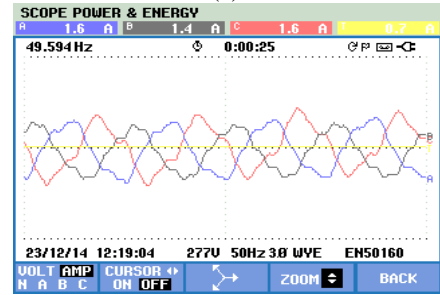


(e)

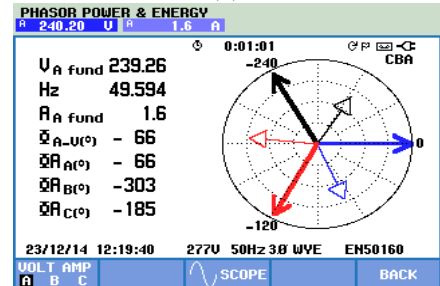
Fig. 16. Measured output parameters of SEIG at rated load of 0.8 lagging power factor (a) three phase load voltages (b) three phase load currents (c) phasors of generated voltage and currents (d) active, reactive and apparent powers and operational power factor (e) load voltage harmonics.



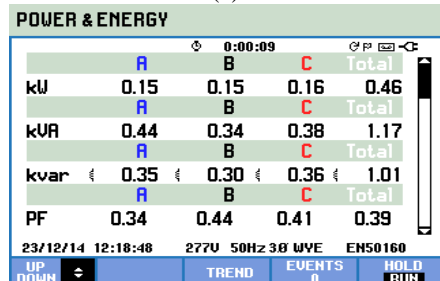
(a)



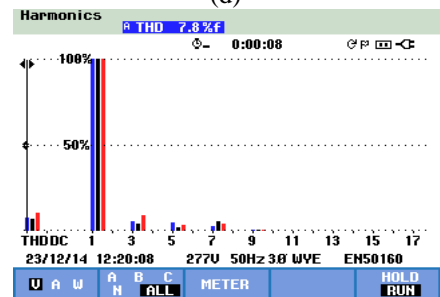
(b)



(c)



(d)



(e)

Fig. 17. Measured output parameters of SEIG feeding a loaded three phase induction motor (dynamic load) (a) three phase load voltages (b) three phase load currents (c) phasors of load voltage and currents (d) active, reactive and apparent powers and operational load power factor (e) load voltage harmonics.

Table 2. Measured output parameters of SEIG.

Type of Load	Phase Voltages			Phase Currents			P	Q	S	%THD of Load voltage
	A	B	C	A	B	C	Cumulative			Cumulative
Unity PF	241	260	247	3.1	2.9	3.0	2.25	0.12	2.27	6.4
0.9 pf lagging	270	277	276	3.2	2.8	3.0	2.24	0.98	2.46	7.4
0.8 lagging	285	284	293	3.5	3.1	3.4	2.36	0.81	2.92	10.8
Dynamic Loading	239	235	237	1.6	1.4	1.6	0.46	1.01	1.17	7.8

6. Conclusion

Detailed dynamic and steady state modeling of a three phase self excited induction generator along with an extensive experimental testing on an open stator winding SEIG is presented. The developed mathematical models are implemented through Matlab using symbolic programming and simulink modeling utilities. The dynamic results reveal SEIG characteristics during transient conditions such as self excitation and voltage buildup as well as effect of step loading of different power factor loads. Voltage buildup with regards to two different pre conditions of remnant charge being derived from rotor and excitation capacitance is analyzed.

For the investigated machine it is found that voltage tends to build-up quicker when the self excitation is initiated from the initial charge on excitation capacitance. For the loads of unity, 0.9 lagging and 0.8 lagging the SEIG is able to supply rated power without any major issues. With lagging power factor loads, however, it is observed that load voltage is increasing with increasing load after going into a certain minima. This dip in voltage is found to be increasing with decreasing lagging power factor of load. Such a profile of load voltage for lagging pf loads is due to the inception of resonance in the SEIG circuit. Also, the increasing load voltage of SEIG for lagging pf loads can be brought within permissible limits by reducing the series capacitance through single stage switching. The steady state results provide detailed insights of different SEIG parameters as the generated voltage varies from no-load to full load for three power factors. Power quality analysis of the generated SEIG parameters is carried out for static as well as dynamic loads through a power and energy analyzer. SEIG is able to supply different category of loads with reasonable degree of satisfaction.

APPENDIX-I

Magnetizing Characteristics of SEIG:

$$V_g/f_{pu} = a1 * X_m^2 + a2 * X_m + a3$$

(for steady state analysis)
 a1 = -0.022011; a2 = 10.324; a3 = -784.11

$$L_m = b1 * I_m^4 + b2 * I_m^3 - b3 * I_m^2 + b4 * I_m + b5$$

(for dynamic model)
 b1 = -0.059126, b2 = 0.41178, b3 = -0.86791, b4 = 0.40901, b5 = 1.0792.

Appendix-II

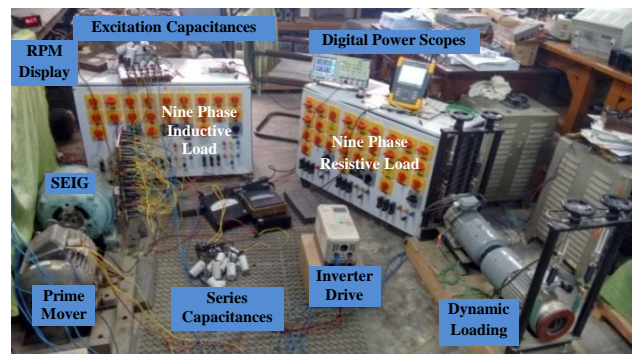


Fig. A1. Three phase SEIG test rig

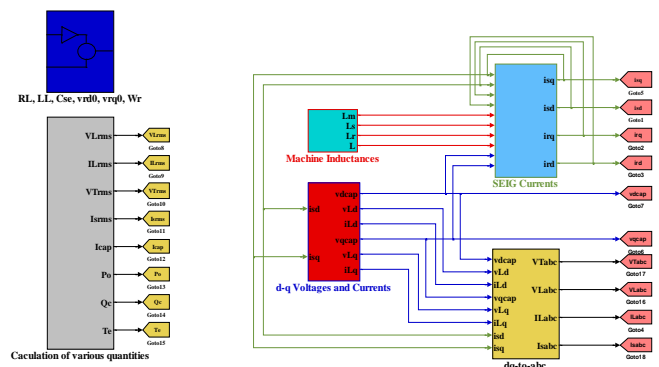


Fig. A2. Simulink model of 3 phase SEIG.

Parameters of prime mover

3-phase, Delta connected, 415 V, 7.6 A, 3.7 KW, 1430 rpm, 50 Hz, Squirrel caged induction motor.

Parameters of inverter drive (Speed Controller)

Yaskawa V1000 AC Drive, 3phase, 2.2 KW, 400V.

Parameters of SEIG

Open stator winding, star connected, squirrel caged, 3 hp, 400 V, 5.5 A, $R_s=12.6 \Omega$, $R_r=15.1 \Omega$, $L_{ls}=0.0640$, $L_{lr}=0.0640$.

Parameters of Load

R-Load : 1.5 KW X 3 (each having 10 steps of 0.150 KW)
L-Load : 180 mH X 3 (each with steps of 12,24, 30,60,90m ,120,180 mH)
Dynamic Load : 3 phase induction motor, 400V 1hp, 1.8 A.

REFERENCES

- [1]. I.P. Girsang, J. S. Dhupia, E. Muljadi, M. Singh, L. Y. Pao, "Gearbox and drive train models to study dynamic effects of modern wind turbines", IEEE Trans. on Ind. Appl. Vol. 50, No. 6: pp. 3777-3786, 2014.(Article)
- [2]. M. F. Khan, M. R. Khan, "Wind Power Generation in India: Evolution, Trends and Prospects", International Journal of Renewable Energy Development, Vol.2, No.3, 2013. (Article)
- [3]. R. C. Bansal, "Three-phase self-excited induction generators-an overview", IEEE Trans. on Ene. Conv. Vol. 20, No. 2, pp.292-299, 2005. (Article)
- [4]. T. F. Chan, "Steady-state analysis of self-excited induction generators. IEEE Trans. on Ene. Conv., Vol.9, No.2, pp.288-295, 1994. (Article)
- [5]. M. H. Haque, "A novel method of evaluating performance characteristics of a self-excited induction generator", IEEE Trans. on Ene. Conv., Vol. 24, No. 2, pp. 358-365, 2009. (Article)
- [6]. T. F. Chan, "Analysis of self-excited induction generator using an iterative method", IEEE Trans. Ener. Conv., vol. 10, no. 3, pp. 502-507, Sep 1995. (Article)
- [7]. S. M. Alghuwainem, "Steady state analysis of self excited induction generator including transformer saturation", IEEE Trans. on Ener. Conv., vol.14,no.3, pp. 667-672, Sep 1999. (Article)
- [8]. P. C Krause, O. Wasynczuk, S. D. Sudhoff, "Analysis of electric machinery and drive systems", IEEE Press, 2002.(Book)
- [9]. C. Grantham, D. Sutanto, B. Mismail, "Steady-state and transient analysis of self-excited induction generators", IEE Proc, vol. 136, pt. E, no. 2, pp.61-68, March 1989.(Article)
- [10]. D. Seyoum, C. Grantham, M.F. Rahman, "The dynamic characteristics of an isolated self-excited induction generator driven by a wind turbine," IEEE Trans. on Ind. Appl., vol.39,no.4,pp.936,944,July-Aug.2003. (Article)
- [11]. M. Bhasker Palle, M. Godoy Somoos and A. Farret Felix, "Dynamic simulation and analysis of parallel self-excited induction generator for island wind farm systems", IEEE Trans. on Ind. Appl., vol 41, no. 4, pp. 1099-1106, 2005.(Article)
- [12]. L.A.C Lopes, R.G, Almeida, "Wind-driven self-excited induction generator with voltage and frequency regulated by a reduced-rating voltage source inverter," IEEE Trans. on Ene. Conv., vol.21, no.2, pp.297,304, June 2006.(Article)
- [13]. T. Ahmed, O. Noro, E. Hiraki, M Nakaoka, "Terminal Voltage Regulation Characteristics by Static Var Compensator for a Three Phase Self-Excited Induction generator." IEEE Trans. on Ind. Appl. vol. 40, no. 4, pp. 978-988, Jul/Aug 2004.(Article)
- [14]. B. Singh, S.S, Murthy, R.S.R. Chilipi, "STATCOM-Based Controller for a Three-Phase SEIG Feeding Single-Phase Loads," IEEE Trans. on Ene. Conv., vol.29, no.2, pp.320,331, June 2014.(Article)
- [15]. R.R., Chilipi, B. Singh, S.S.Murthy, "Performance of a Self-Excited Induction Generator With DSTATCOM-DTC Drive-Based Voltage and Frequency Controller," IEEE Trans. on Ene. Conv., vol.29, no.3, pp.545,557, Sept. 2014.(Article)
- [16]. Li. Wang; Dong-Jing Lee, "Coordination Control of an AC-to-DC Converter and a Switched Excitation Capacitor Bank for an Autonomous Self-Excited Induction Generator in Renewable-Energy Systems," IEEE Trans. on Ind. Appl., vol.50, no.4, pp.2828-2836, July-Aug. 2014.(Article)
- [17]. MATLAB® Version 7.10.0.499 (R2010a). The MathWorks, Inc, US.
- [18]. B. Singh, M. Singh, A.K. Tandon, "Transient Performance of Series-Compensated Three-Phase Self-Excited Induction Generator Feeding Dynamic Loads," IEEE Trans. on Ind. Appl., vol.46, no.4, pp.1271,1280, July-Aug. 2010.(Article)
- [19]. M.F Khan, M.R. Khan, "Self regulating three phase-self excited induction generator for standalone generation," in Proc. IEEE INDICON 2013, pp.1-6, 13-15 Dec. 2013. (Conference Paper)
- [20]. M. Abdel-Halim, Al-Ahmar M. A. and El-Sherif M. Z, "A novel approach for the analysis of self-excited induction generators", Elec. Mach. & Pow. Sys, vol. 27, pp. 879-888, 1999.(Article)
- [21]. N. Ammasaigounden, Subbiah M., and Krishnamurthy M. R, "Wind-driven self- excited pole changing induction generators", Proc. Inst. Elect. Eng. B, vol. 133, no. 5, pp. 315-321, 1986.(Article)
- [22]. N. Malik, A. Maxi, "Capacitance Requirements for Isolated Self-Excited Induction Generators," IEEE Trans. on Ene. Conv., vol. 2, no. 1, pp. 62-69. 1987. (Article)
- [23]. Kalamen Luká's, Rafajdus Pavol, Sekerák Peter, and Hrabovcová Valéria, "A novel method of magnetizing inductance investigation of self-excited induction generator", IEEE Trans. on Magnetics, vol. 48, no. 4, pp. 1657-1660, April 2012.(Article)
- [24]. M. R. Khan, M. F. Khan, A. Iqbal, "Investigation on Resonating Behaviour of a Self Excited Induction Generator", in Proc. IEEE Tencon-Spring, 2013, 16-19 April 2013, Sydney, Australia.(Conference Paper)